www.czasopisma.pan.pl PAN POLSKA AKADEMIA NAUK www.journals.pan.pl

Arch. Min. Sci. **64** (2019), 4, 655-670

Electronic version (in color) of this paper is available: http://mining.archives.pl

DOI 10.24425/ams.2019.129375

BEI-FANG WANG*,**,****#, KE-MING SUN***,
BING LIANG***, WEI-JI SUN***

DEVELOPMENT AND APPLICATION OF AN EXPERIMENTAL DEVICE FOR MEASURING STORAGE COEFFICIENT IN A COAL MINE UNDERGROUND RESERVOIR

OPRACOWANIE I ZASTOSOWANIE EKSPERYMENTALNEGO URZĄDZENIA DO POMIARÓW WSPÓŁCZYNNIKA ODSĄCZALNOŚCI W PODZIEMNYCH ZBIORNIKACH WODY W KOPALNIACH WĘGLA

With the rise of coal mine underground reservoir engineering in the Shendong Mining Area, the space time dynamic evolution prediction of storage coefficient is becoming one of the critical technical problems for long-term reservoir operation. This coefficient directly determines the storage capacity and the comprehensive benefits of the operation of a coal mine underground reservoir. To this end, the proposed underground reservoir in Daliuta coal mine (No. 22616 working face) is selected in this study for the development and application of an experimental device to measure the storage coefficient. Rock and coal fragments from similar materials are prepared, which are filled and loaded according to the caving rock nature as well as the lumpiness and accumulation mode characteristics pertaining to No. 22616 working face. Subsequently, the measured storage coefficient under circulating water injection conditions revealed a four-dimensional spatial and temporal pattern. It followed the law of storage coefficient under joint interaction of water-rock and stress. The results showed that, prior to the experiment, rock and coal fragments made from similar materials had good water resistance when the paraffin content was set at 8%. The three stress zones were defined based on a theoretical analysis, which were applied on the corresponding loads. During the experiments, significant regional differences were found in the top surface with persisting subsidence of each stress loading zone. Hence, compared with its initial state, the maximum subsidence in the stress stability zone, the stress recovery zone, and the low-stress zone was 7.89, 5.8, and 1.83 mm, respectively. While the storage capacity and the storage coefficient gradually decreased, the former ranged from 0.2429 to 0.2397 m^3, and the latter ranged from 0.270 to 0.266. The experimental results are verified by drainage engineering tests in the Shendong Mining Area. In essence, the storage coefficient had remarkable spatial distribution characteristics and a time-varying effect. In space, the storage coefficient increased with height along the vertical direction of the coal mine underground reservoir. However, it decreased with the distance from the boundary of the dam body in the horizontal direction.

* SCHOOL OF MINES, LIAONING TECHNICAL UNIVERSITY, FUXIN 123000, PR CHINA
** STATE KEY LABORATORY OF COAL RESOURCES AND SAFE MINING, CHINA UNIVERSITY OF MINING AND TECHNOLOGY, XUZHOU 221008, PR CHINA
*** SCHOOL OF MECHANICS AND ENGINEERING, LIAONING TECHNICAL UNIVERSITY, FUXIN 123000, PR CHINA
**** STATE KEY LABORATORY OF WATER RESOURCE PROTECTION AND UTILIZATION IN COAL MINING, BEIJING 100011, PR CHINA)

\# Corresponding author: wang_beifang@126.com

With time, the storage coefficient decreased dynamically. This study provides a new way of predicting the storage coefficient of a coal mine underground reservoir.

Keywords: coal mine underground reservoir; rock and coal fragments made from similar materials; partition loading; water-rock interaction; storage coefficient; space time dynamic evolution

Przy rosnącej intensywności prac inżynieryjnych prowadzonych w rejonie Zagłębia Węglowego w Shendong, określanie współczynnika odsączalności i jego zmienności w czasie i przestrzeni stało się jednym z głównych problemów w długofalowej eksploatacji górniczej, mającej wpływ na kształtowanie się współczynnika odsączalności oraz na całościowe korzyści płynące z eksploatacji złoża. Zaproponowano by rejon prac wydobywczych prowadzonych w ścianie No 22616 w kopalni węgla Daliuta wykorzystany został jako teren eksperymentalny dla pomiarów współczynnika odsączalności dla zbiornika podziemnego znajdującego się w kopalni węgla. W tych warunkach przetestowano opracowane narzędzie pomiarowe. Do eksperymentu przygotowano fragmenty skał i węgla o podobnym składzie jak w rejonie ściany 22616, z zachowaniem ich układu zalegania i zwięzłości; następnie obciążono je w sposób analogiczny do obciążeń działających w warunkach rzeczywistego prowadzenia stropu. Dokonano pomiaru współczynnika odsączalności po wpompowaniu do próbek wody, w rezultacie uzyskując czterowymiarowy rozkład współczynnika odsączalności w czasie i przestrzeni w warunkach wzajemnych oddziaływań pomiędzy wodą a warstwami skał, oraz w warunkach działających naprężeń. Wyniki eksperymentu były następujące: Przed rozpoczęciem eksperymentu, wykorzystywane fragmenty skał i węgla charakteryzowały się wysoką odpornością na wodę gdy zawartość parafiny wynosiła 8%; następnie trzy obszary próbek wyodrębnione w oparciu o analizy teoretyczne i charakteryzujące określony poziom naprężeń poddano wielokrotnemu działaniu naprężeń o kontrolowanej wielkości. W trakcie trwania eksperymentu zaobserwowano znaczące różnice lokalne na powierzchni, w postaci utrzymującej się niecki osiadania nad poszczególnym strefami oddziaływania naprężeń. W porównaniu do stanu początkowego, maksymalne wartości osiadania w strefie stabilnych naprężeń, w strefie odprężenia i w strefie niskich naprężeń wyniosły odpowiednio: 7.89 mm, 5.8 mm i 1.83 mm. Współczynnik odsączalności stopniowo malał, od początkowego zakresu 0.270-0.266 do zakresu końcowego 0.2429 m^3-0.2397 m^3. Wyniki badań eksperymentalnych potwierdzone zostały następnie poprzez badania odprowadzania wody przeprowadzone w rejonie Zagłębia Węglowego Shendong. Stwierdzono, że współczynnik odsączalności wykazuje znaczną zmienność w czasie i przestrzeni. W ujęciu przestrzennym, wartość współczynnika odsączalności wzrasta wraz z wysokością mierzoną w kierunku pionowym osi zbiornika podziemnego, z kolei maleje ona wraz z odległością od granicy tamy mierzonej w kierunku poziomym. W ujęciu czasowym, wartość współczynnika odsączalności gwałtownie rośnie w czasie. Badania powyższe dostarczyły nowych metod do prognozowania wartości współczynnika odsączalności w podziemnych zbiornikach na terenie kopalni węgla.

Słowa kluczowe: podziemny zbiornik w kopalni, fragmenty skał i węgla o podobnym składzie jak w rejonie ściany, obciążenie stopniowe, wzajemne oddziaływania wody i skał, współczynnik odsączalności, dynamiczny rozkład czasowo- przestrzenny

1. Introduction

To address the increasing water scarcity problems associated with large-scale developments in the arid and semi-arid mining areas in western China, a method of storing and utilising mine water by using a coal mine underground reservoir is proposed in the Shendong mining area. A fully used caving rock void in goaf formed after the completion of a coal mining operation can provide a storing space. The coal pillars connected by artificial construction can serve as a dam body, where natural filtration and purification through caving rocks may allow for the

cyclic utilisation of water by means of equipping it with water injection and water intake facilities. Such developments can effectively alleviate the water shortage problem around the mine area (Gu et al., 2016; Fan et al., 2015). However, many technical problems are encountered in the process of coal mine underground reservoir engineering construction and operation. Such problems include site selection, storage design, dam construction, network building, and water quality protection and monitoring. In particular, storage coefficient measurement in the design of a storage system is one of the most important problems as it directly determines the storage capacity and the comprehensive benefit of operating a coal mine underground reservoir.

For this purpose, significant research has been conducted by both domestic and foreign scholars. Chinese scholar Luo (2010) constructed a water accumulation coefficient prediction model in goaf with a nonlinear theory based on water accumulation data in a mined-out area in the Huainan coalfield. However, the time-dependency was not considered in this work. Gu et al. (2015) first mentioned the concept of storage coefficient in coal mine underground reservoirs, who established a capacity calculation model. Sufficient consideration was given to the dynamic characteristics of the storage coefficient. However, related parameter acquisition is deemed inconvenient to calculate. Gao et al. (2015) noted the correlation between the storage coefficient and the water level in a typical coal mine underground reservoir. This work adopted the stratified accumulation method to calculate the capacity, which is simple to calculate and yields good output results. However, the results were affected significantly by the altitude interval. Peng et al. (1994) used the water absorption and void ratio of caving rocks to calculate the water storage rate in a goaf. This effectively overcame the challenging issue with caving rock where the void volume was quantified. However, the errors in the output results were relatively high. The foreign scholars mainly conducted investigations on the storage coefficient of aquifers. Indian scholars Ballukraya et al. (1991) determined the storage coefficient according to the residual drawdown of an observation well in a confined aquifer. Sahni et al. (1979) measured the storage coefficient of an underground aquifer in light of a pressure contour map. Scholars from Thailand, Arlai et al. (2012), brought forward a dynamic prediction model for the storage coefficient of an underground aquifer in Thailand applying various relevant parameters of groundwater development. Although these methods possessed distinct computing advantages, there were some limitations in their scope of application. Spanish scholars Ordóñez et al. (2015) established a prediction model for water replenishment from a river in a mine goaf of Austrian Central Coal Basin. However, the water storage coefficient was not involved.

In summary, scholars at home and abroad generally applied the combined method of mathematical modelling and field measurements to predict the storage coefficient of underground reservoirs. However, the experimental investigations are extremely rare. Simultaneously, the past investigations on storage coefficient basically had fixed values, where time and space dynamic evolution under the interactions of water-rock were mostly ignored. This seriously affected the prediction accuracy. In this connection, an experimental device for measuring the storage coefficient of coal mine underground reservoir is developed in our work. A proposed underground reservoir in Daliuta coal mine (No. 22616 working face) is selected for this study to predict the storage coefficient of the coal mine underground reservoir. Tests were conducted using field monitoring, which provided an important theoretical basis for the design of the storage system and for planning the operation of the coal mine underground reservoir.

2. Experimental device development

The rock void in goaf is to be used as the storage space inside the coal mine underground reservoir. Therefore, the storage capacity is mainly determined by the rock void volume in the caving zone of the goaf. It is difficult to measure the void volume directly because of the irregular shape and distribution of the caving rock. However, the storage capacity can be predicted indirectly through the storage coefficient of the coal mine underground reservoir. The storage coefficient is one of the most important parameters to measure the storage capacity of the coal mine underground reservoir. This is a representation of the spatial proportion of the caving zone rock void in goaf. This primarily depends on the rock void ratio in the caving zone of the goaf. It is closely related to the mining technology, mining pressure, caving rock nature, and lumpiness and accumulation mode. It is characterised by dynamic changes and gradual stabilisation with time. Considering the above factors, an experimental device for measuring the storage coefficient of the coal mine underground reservoir is independently developed. This scheme is shown in Figure 1.

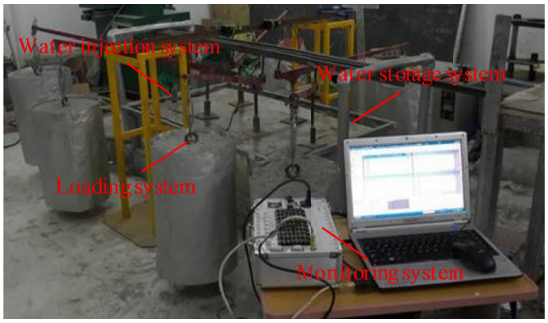

Fig. 1. Experimental device for measuring the storage coefficient of the coal mine underground reservoir

The experimental device consisted of four fundamental systems: water injection system, water storage system, loading system and monitoring system. These are described below:

(1) Water injection system

The water injection system is composed of a water tank, water pump, water pipe, and valve. The water tank has a volume of 100 l and helps perform transfer water injection. It is placed on the bracket to increase the potential energy of the water. Its top part is connected to the water inlet pipe to realise a real-time replenishment mechanism. The water pump is set at the bottom of the water tank. This is a model QB80/750W vortex pump, with a power consumption rating of 0.75 kW, a maximum lift of 55 m, and a maximum flow of 50 l/min. The water pipe diameter is 32 mm. The water control valve regulated the water injection flow.

(2) Water storage system

The water storage system is composed of a metal trough and rock and coal fragments made from similar materials. The metal trough simulated the space of a caving zone in the goaf, which has dimensions of 1.5 m×1 m×0.6 m (length, width and height). Its volume is 0.9 m^3. Rock and coal fragments made from similar material fragments are prepared and filled on the grounds of the rock nature, reflecting the lumpiness and accumulation mode of the caving zone in the goaf.

(3) Loading system

The loading system is composed of a weight, a lever, and a pressing plate. The loading lever is the labour-saving lever. The ratio of power to resistance is 1:10. The front end of the lever is hinged on the fixed bar above the metal trough as the fulcrum of the loading lever. The point 0.1 m from the front end of the lever is connected with the pressing tray. Therefore, the lever load could pass through the pressing tray to the pressing plate that is divided based on the caving zone rock stress distribution in the goaf. A weight is hung at the back end of the lever. This weight is varied according to the stress similarity ratio. In this way, the partition of load that has a similar material as the rock and coal fragments is realised.

(4) Monitoring system

The monitoring system is composed of displacement monitoring equipment, a water injection measuring equipment, and a computer. A M1L/100 of laser displacement sensor is used as the displacement monitoring equipment. This is set on the fixed bar above the metal trough, which is not attached to the object surface. It belongs to an analogue triangulation mechanism without using additional electronic units. The measurement frequency is 100/s, and the measurement range is 100 mm. A CDI-C06 turbine flowmeter is used as the water injection measuring equipment. This is placed at the water inlet and water outlet. The device calibre is 32 mm, and the flow range is 10-100 l/min.

3. Experimental device application

(1) Engineering background

At present, Daliuta coal mine has entered its final mining stage. The Upper group coal, and the main coal seam of the Lower group coal has become the main mining coal seam in the entire mine. To promote mining with water resource conservation, combined with geological conditions and economic factors, underground reservoir related theory and experience are being utilised to build a coal mine underground reservoir. The locations are the fourth panel, old sixth panel, sixth panel goaf of No. 2^{-2} coal seam and third panel goaf of No. 5^{-2} coal seam. Subsequently, mine water produced during mining is injected into these goaves. This water is to be extracted after adsorption, filtration, and purification through the caving rock. This is essentially a scheme for mine water recycling. The No. 22616 fully mechanised coal face is being proposed as the underground reservoir. This area is selected for this study. The storage coefficient measurement experiment is located at the sixth panel of the first level, main mining No. 2^{-2} coal seam with a buried depth of 41.82-96.43 m, thickness of 5.3 m, and dip angle of 1°-3°. The structure is relatively simple. A retreating-longwall mining method and "three shifts" operation method are adopted in the face. A 7LS6/LWS536 coal winning machine is used to cut the coal, 3×1000 kW scraper conveyors are used to carry the coal, a ZY11000/24/50 hydraulic support is used to control the roof, and a total caving method is used to manage the roof with a caving zone height of 15 m for the goaf.

(2) Experimental method

A certain volume of metal trough is chosen to simulate the caving zone space in the goaf of No. 22616 working face. The rock and coal fragments made from similar materials are prepared, filled, and loaded according to the caving rock nature as well as the lumpiness and accumulation mode characteristics. After the compacted rock and coal fragments made from similar materials

are stabilised, mine water is injected into the metal trough, and the storage coefficient is measured. When the water injection level is approximately parallel with the top surface of the loading rock and coal fragments made from similar materials, the ratio of the injected water volume to the iron trough volume is calculated as the storage coefficient of the coal mine underground reservoir.

- Specimen preparation
  a. Field sampling
     Based on the mine geological data, caving zone rock in goaf of No. 22616 working face mostly comprise sandstone, mudstone, and a small amount of residual slack coal. Thereinto, a thin layer of residual slack coal is covered on the goaf bottom and some mudstone is spread in the middle and lower parts of the goaf. Moreover, a large amount of sandstone is filled in the upper and middle parts of the goaf. The measured rock lumpiness (sandstone and mudstone) and the calculated lumpiness proportion are shown in table 1. Based on the regulation of the PRC standard GB/T23561.1-2009, to estimate the caving rock mixing ratio in the goaf, rock, and coal, samples are collected from the working face having a similar ratio. The total weight is 100 kg. To obtain No. 2^{-2} coal seam physical and mechanical parameters, No. 2^{-2} coal seam samples are also taken.

TABLE 1

Caving rock lumpiness and proportion in goaf of No. 22616 working face

Lumpiness (m)	Proportion
>5	5%
5-3.75	10%
3.75-2.5	15%
1.25-2.5	25%
0-1.25	45%

In the same way, complying with the regulations of PRC standard GB/T23561.1-2009, physical and mechanical properties are determined using tests on collected rock and coal samples. These are conducted under natural and soaking states. The results are shown in Table 2. Once the rock and coal are soaked with mine water, it would expand rapidly and subsequently disintegrate and soften. Therefore, its mechanical properties

TABLE 2

Physical and mechanical parameters of rock and coal

Lithology	State	Density P (g·cm^{-3})	Compressive strength σ_c (MPa)	Tensile strength σ_t (MPa)	Cohesion C (MPa)	Friction Φ (°)	Elasticity modulus E (GPa)	Poisson's ratio μ
Sandstone	Nature	2.39	46.20	6.90	8.20	42	45.00	0.27
	Soaking	2.39	40.49	4.67	6.51	41	42.75	0.29
Mudstone	Nature	2.45	39.90	4.00	3.20	35	11.00	0.30
	Soaking	2.44	31.71	2.80	2.54	33	6.38	0.33
Coal	Nature	1.30	10.50	0.75	1.60	38	15.00	0.35
	Soaking	1.28	8.69	0.42	1.27	37	10.99	0.37

greatly weaken under the long-term comprehensive action of the physical, chemical, and stress (Oda et al., 2002; Noiriel et al., 2010; Watanabe et al., 2011) conditions. Compared with the natural rock and coal, the soaking rock and coal's mechanical properties are decreased by 20.52%.

b. Material mixture ratio

To satisfy the requirements, apart from having very weak permeability and hygroscopicity, rock and coal fragments made from similar materials should also be of suitable strength. They should not be loose under long-term mine water leaching conditions. Combined with rock and coal mechanical properties, river sand is selected as the aggregate. Calcium carbonate and gypsum are selected as the cemented material. Paraffin is considered as the water resistant modified material to prepare the waterproof rock and coal fragments made from similar materials (Huang et al., 2010; Wang et al., 2016; Fan et al., 2016). This is shown in Figure 2. With the given permeability and hygroscopicity, the change laws of rock and coal fragments (made from similar material with sand, calcium carbonate and gypsum as the raw material) are relatively similar. The hygroscopicity of rock and coal fragments made from similar materials has been well studied and was proven to meet the requirements, such as those in (Lian et al., 2015). Only the mechanical strength and permeability need to be studied. However, the combination of gypsum and paraffin could effectively control the mechanical strength and the permeability of the similar materials. Gypsum, as a cementing agent, has a strong cementing effect on the fine aggregate and a weak disintegrating characteristic upon contacting water. Paraffin, as a non-hydrophilic oily regulator, fully mixed with fine aggregates and filled in the pores of a coarse aggregate; thus, it not only blocks the seepage channel but also withstands the water pressure. Therefore, paraffin is selected to adjust the water resistance of the similar materials.

Fig. 2. Raw material of the examined materials

Part of the rock and coal fragments made from the similar materials were selected to dip in the mine water before the experiment is conducted to explore the relationship between the paraffin content and the rock and coal fragments made from similar

materials. There is no need for examination when the paraffin content in the sample is 0, because it would dissolve immediately in the mine water. Therefore, the paraffin content is set to 5-10%. The sample's compressive strength and penetration rate are tested after dipping them in mine water for 24 h. It can be seen from Figure 3 that the compressive strength of the rock and coal fragments made from the similar materials increased with the increase of the paraffin content, while the penetration rate decreased.

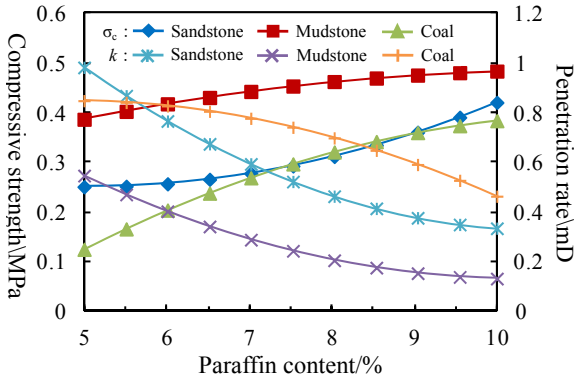

Fig. 3. Relationship between paraffin content and the similar materials' properties

However, when the paraffin content exceeded 8%, the compressive strength and the penetration rate variation of the samples both tended to be consistent. Therefore, 8% of paraffin content is an important control node for the mechanical strength and permeability of the rock and coal fragments made from similar materials. In the end, the material mixture ratios of rock and coal fragments made from similar materials are determined through a large number of matching experiments. These are shown in Table 3.

TABLE 3

Rock and coal fragments made from similar materials mixture ratio

Similar material	River sand: Calcium carbonate: Gypsum	Paraffin/%	Water/%
Sandstone	7:5:5	8	12
Mudstone	7:6:4	8	12
Coal	9:7:3	8	12

c. Gradation set

To simulate the rock occurring state in the caving zone of the goaf to a maximal degree, the rock and coal fragments made from the similar materials are prepared and filled in strict accordance with the caving rock nature, lumpiness, proportion, and spatial distribution. Based on the proportional relation between the metal trough height of 0.6 m and the caving zone height of 15 m, the geometric similarity ratio is set to 1:25, and the strength similarity ratio is set to 1:37.

Fig. 4. Lumpiness of rock and coal fragments made from similar materials

In this way, the rock and coal samples made from the similar materials are prepared according to the rock and coal actual strength, lumpiness and proportion. The rock samples made from the similar materials are broken into slack, and the coal samples made from the similar materials are broken into fragments. As shown in Figure 4, 0-5 cm lumpiness proportion is 45%, which contains sandstone and mudstone made from similar materials. While lumpiness greater than 5 cm is observed for all sandstone made from the similar materials, 5-10 cm lumpiness proportion was 25%, 10-15 cm lumpiness proportion was 15%, 15-20 cm lumpiness proportion was 10%, and more than 20 cm lumpiness proportion was 5%. Referring to the rock spatial distribution in the caving zone of the goaf (see Fig. 5), slack coal made from the similar materials is filled in the bottom of the metal trough, mudstone fragments made from the similar materials are filled in the lower part of metal trough, and sandstone fragments made from the similar materials are filled in the upper part of metal trough.

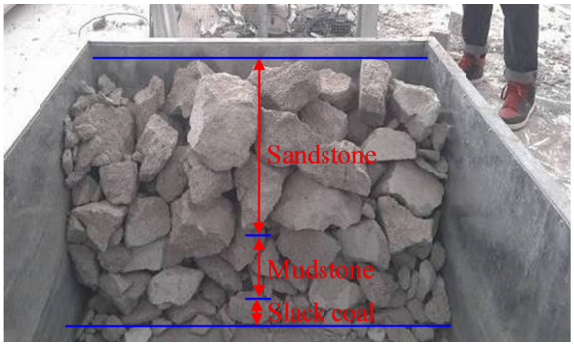

Fig. 5. Rock and coal fragments made from the similar material filling

- Partition load
  The caving rock stress primarily comes from the overburden pressure of the goaf, due to forming a cantilever beam structure in the overlying strata close to the coal wall. The stress effect of the overburden on the caving rock is restricted. A periodic weighting area

coverage near the goaf border is called the low stress zone, where caving rock stress is significantly lower than other areas (Campoli et al., 1993). Referring to Wilson's research (1983), away from the coal wall at 0.3 H range (H is the buried depth) in the goaf, the region is called a stress recovery zone. Here, the overlying strata generally sank and formed a step rock beam structure. Therefore, only a part of the pressured rock mass acted on the caving rock, and the caving rock stress gradually recovered (King et al., 1970; Yavuz, 2004). The middle region of the goaf is called the stress stability zone. Here, because of the step rock beam structure failure, the caving rock is completely compacted by the overlying strata, which is basically in the original rock stress state (Wang et al., 1993; Liang et al., 2016; Wang et al., 2017). This is shown in Figure 6. On the grounds of the caving rock stress partition in goaf of No. 22616 working face, the partition loading is implemented to the rock and coal fragments made from the similar materials in the metal trough with geometric similarity ratio of 1:25, and stress similarity ratio of 1:37. A stress of 0 MPa is determined as the low stress zone load, 0.9 MPa is determined as the stress recovery zone load, and 1.8 MPa is determined as the stress stability zone load according to the ground pressure field measured data in the goaf.

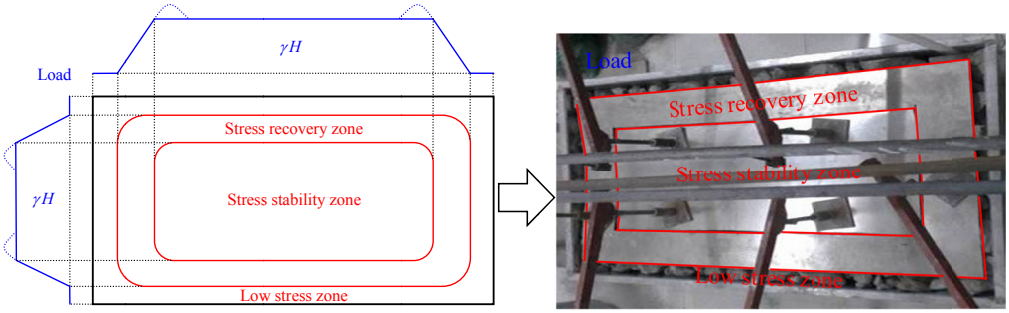

a) Stress distribution model b) Stress partition loading

Fig. 6. Caving zone rock stress in goaf of No. 22616 working face

(3) Experimental result

After the rock and coal fragments made from the similar materials are compacted and tended towards stability, mine water is injected into the metal trough with a constant flow rate of 1.3 m^3/h. The water level is observed and the water injection rate is recorded until the water level line flushed with rock and coal fragments made from the similar materials' top surface. In the process of water injection, the water level increased unevenly with time. At the beginning of the water injection, the water level rose rapidly and showed a prominent linear change, with an average rising speed of 145.0 mm/min. This is the linear rapid rising stage of the water level. After water injection lasted for 3 min, the water level rose at a slower rate and showed a remarkable concave-upward curve. The average rising speed was 31.4 mm/min, which is the non-linear rapid rising stage of the water level. After injecting continuously for 9 min, the water level rose slowly and showed a relatively weak change. It was not until 13 min that the metal trough was filled with an average rising speed of 5.5 mm/min, which is the slow rising stage of the water level. This observation is shown in Figure 7.

a) Circulating water injection

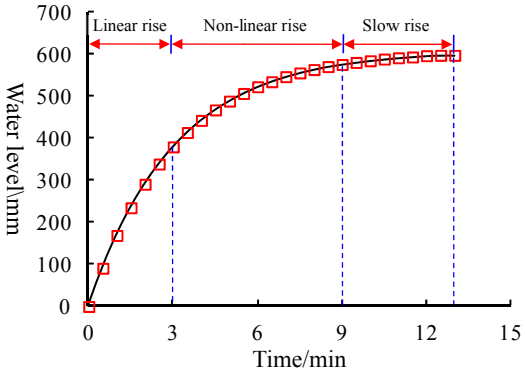

b) Water injection level change curve

Fig. 7. Water injection level observation

The process of mine water cycle storage and utilisation in a coal mine underground reservoir is simulated by constant water injection and water release of the metal trough. The top surface subsidence displacement curve of each stress zone in the metal trough during this period is shown in Figure 8. There was certain distinction in the top surface subsidence displacement of different stress zones. The top surface subsidence displacement of the stress stability zone was the maximum, that of the stress recovery zone was the second, and that of the low stress zone was the minimum. However, the top surface subsidence displacement variation trend of each stress zone was more consistent, and all unevenly decreased with time. In the early-stage experiment (the first 10 h), the top surface subsidence displacement change and the amount of different stress zones were all relatively fast and large, respectively. In the medium-stage experiment (10-30 h), the top surface subsidence displacement change and the amount of different stress zones were all gradually slow and decreasing, respectively. In the late-stage experiment (after 30 h), the top surface subsidence displacement change of different stress zones tended to be stable, and the amount was basically unchanged. Finally, compared with its initial state, the top surface subsidence displacement of

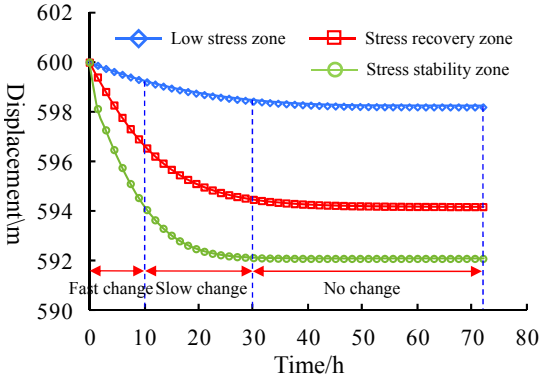

Fig. 8. Different stress zones' top surface subsidence displacement change curves

the stress stability zone was 7.89 mm, with a variation of 1.32%. The corresponding displacement and variation of the stress recovery zone and the low stress zone were 5.81 mm, 0.97%, and 1.83 mm, 0.31%, respectively. In other words, the top surface subsidence displacement change and the amount of different stress zones also had outstanding partition characteristics.

Simultaneously, as each stress zone's top surface subsiding in the metal trough, rock and coal fragments made from similar materials were further compacted, and the storage space of the metal trough continued to be compressed. Therefore, the storage capacity gradually decreased from 0.2429 to 0.2397 m^3. The corresponding subsidence displacement changing process of each stress zone's top surface, and the storage stability changing process are divided into three stages. The first 10 h stage is the storage capacity rapid decrease stage, where the storage capacity decreases from 0.2429 to 0.2409 m^3. The period of 10-30 h is the storage capacity slow decrease stage, where the storage capacity decreases from 0.2409 to 0.2397 m^3. After 30 h, the storage capacity stabilisation stage is attained, where the storage capacity is basically maintained at 0.2397 m^3, as shown in Figure 9.

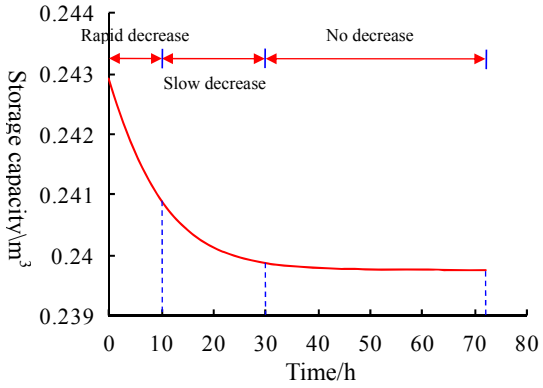

Fig. 9. Metal trough storage capacity change curve

Finally, the ratio of water injection rate to metal trough volume is used to predict the storage coefficient of the coal mine underground reservoir. When the metal trough volume got in line with its length and width, the storage coefficient of the coal mine underground reservoir is calculated by the formula $K = K_{WI}/V_{MI}$. Here, K is the storage coefficient, V_{WI} is the water injection volume, and V_{MT} is the metal trough volume. Similarly, three groups of experiments are repeatedly conducted in accordance with the above steps, and the arithmetic mean value of the three experimental results is taken as the final storage coefficient, as shown in Table 4.

TABLE 4

Storage coefficient measurement

Metal trough	Size (m)	Volume (m^3)	Water injection rate (m^3)	Storage coefficient	Mean value
Length	1.5	0.9	0.2397	0.266	0.266
Width	1.0		0.2384	0.265	
Height	0.6		0.2415	0.268	

4. Analysis and discussion

Considering the characteristics of the caving rock void in a goaf, which acts as the storage carrier in a coal mine underground reservoir, the rock and coal hydroscopicity are not considered in this work. Hence, the storage coefficient mainly depends on the caving rock voidage in the goaf. For the shallow buried coal seams in Shendong Mining area, fully mechanised caving mining technology is commonly and widely applied in a coal mine. Therefore, caving rock voidage in the goaf is affected by many factors, such as mining pressure, rock nature, lumpiness, accumulation mode and time, etc.

It can be seen from Figure 7 that the water level rises non-uniformly during water injected into the metal trough. The main reason being the rock and coal fragments made from similar materials nature, lumpiness, accumulation mode had obvious distribution differences along the vertical direction of the metal trough (the gravity of the rock and coal fragments made from the similar materials are ignored for the moment). The psephicity of the tiny slack coal made from similar materials covered on the bottom of metal trough was good, and the edges and corners were not obvious. Part of the slack coal made from the similar materials was further crushed and were formed into pulverised coal under combined action of mine water and external load. The smaller the slack coal fragmentation made from the similar materials, the less obvious the difference was. In addition, the more difficult it was to constitute skeleton structures, the corresponding slack coal void would be filled by pulverised coal in turn. Therefore, the residual storage space was little and the water injection level rose rapidly. Slightly larger mudstone fragments made from the similar materials spread in the middle and lower parts of the metal trough. These were disintegrated and broken under combined action of the mine water and external load. There were some differences in lumpiness. The larger fragments could form skeleton structures, and the space of the skeleton structure could not be completely filled by the smaller fragments. Hence, the residual storage space became larger and the water injection level slowed down. The strength of the large sandstone fragments made from the similar materials distributed in the upper and middle parts of the metal trough was quite high. Psephicity was severe, and the edges and corners were obvious. It was difficult to deform under the combined action of mine water and external load. Meanwhile a large skeleton structure was easily generated among the large fragments. As a result, there was a large amount of residual storage space, and the water injection level rose slowly.

As observed in Figure 8, a distinct partition phenomenon reflecting the top surface subsidence displacement in different stress zones is obvious in the regional variations of the rock and coal fragments made from the similar materials. Compressive deformation is visible in the horizontal direction of the metal trough under the joint interaction of water-rock and stress. Low stress zone in the metal trough did not have any applied load, where there were plenty of voids. Owing to the loose rock and coal fragments made from the similar materials, the deformations were mainly due to decrease in strength and lumpiness caused by softening and disintegration of mine water. The loose rock and coal fragments made from the similar materials in the low stress zone of the metal trough diminished under water-rock reactions with time. Because it was difficult to restore the original complete state of the broken rock and coal fragments made from the similar materials under compaction conditions, there was still some residual void among the compacted rock and coal fragments made from the similar materials. The deformation resistant capability were always weakened under physical and chemical effects of the mine water (Palchik, 2015; Groccia et al., 2016). Therefore, the rock and coal fragments made from the similar

materials soaked with mine water over the long-term should rotate, move and readjust the contact state under the external load. The residual void of the compacted rock and coal fragments made from the similar materials were further compressed. Early on, under the joint interaction of the water-rock and stress, the deformation resistant capability of the rock and coal fragments made from the similar materials were relatively weak, and the residual void was closed rapidly, which decreased linearly with time. After the observed compressing deformation in the early stage, the compacted rock and coal fragments made from the similar materials' density increased quickly and continuously, and the edges and corners locked each other to form more compact skeleton structures that had certain carrying capacity This enhanced the deformation resistant capability. In addition, it would take longer to compress the residual void under the joint interaction of water-rock and stress. When the unceasingly weakening strength of the rock and coal fragments made from the similar materials was exceeded by the external load, these would break and fill the residual void. The residual void's decreasing amplitude gradually diminishes, which shows a clear concave-downward trend. However, the skeleton structure of the rock and coal fragments made from the similar materials are further reinforced under long-term joint interaction of water-rock and stress. The residual void is filled to close, loose medium property of the rock and coal fragments made from the similar materials gradually disappears and transforms into continuous medium until the residual void's compressing deformation tends to stabilise. Finally, for a given stress partition feature in the metal trough, the compaction degree of the rock and coal fragments made from the similar materials in stress stability zone is greater than that of the stress recovery zone and the low stress zone under joint interaction of water-rock and stress. This indicates that the storage coefficient of the coal mine underground reservoir is badly affected by the joint interaction of water-rock and stress. From Figure 8 we can see that the residual void compressed deformation of the rock and coal fragments made from the similar materials in the metal trough also has certain time-dependant characteristic. In addition to the prominent spatial distribution features, as explained in Figure 9, the dynamic change in storage capacity in terms of the storage coefficient can also be observed.

Based on the above analysis, it can be concluded that the storage coefficient of a coal mine underground reservoir has remarkable spatial distribution characteristics and time changing effects. In space, the storage coefficient increases with height along the vertical direction of the coal mine underground reservoir, while decreases with the distance from the boundary dam body in the horizontal direction. In time, the storage coefficient dynamically decreases with time. Therefore, the storage coefficient of a coal mine underground reservoir has significant spatial-temporal features. It is concluded that the storage coefficient of a coal mine underground reservoir was generally approximately 0.30 from the drainage engineering test in the Shendong Mining Area. This is close to the experimental result of 0.266. This verifies the feasibility of the experiments for measuring the storage coefficient in a coal mine underground reservoir. This also provides a new way for predicting the storage coefficient of a coal mine underground reservoir.

5. Conclusion

(1) Based on the similarity principle and the coal mine underground reservoir's storage characteristics, No. 22616 working face (the proposed underground reservoir in Daliuta coal mine) had been selected for study in this work. We independently developed an experimental device for measuring the storage coefficient of the coal mine underground reservoir. The material mixture

ratio of waterproof rock and coal fragments made from similar materials was selected. Two key technical problems were successfully solved, paraffin was chosen as the water resistant adjusting material and its content was set to 8%. In addition, three stress loading zones were designated, where the low stress zone load was 0 MPa, the stress recovery zone load was 0.9 MPa, and the stress stability zone load was 1.8 MPa.

(2) During the circulating water injection in experiment, in the early stages of water injection, the water level rose unevenly with time. After a while, with the regional distinction of the top surface subsidence displacement in the different stress zones, he top surface subsidence maximal displacement of the stress stability zone was 7.89 mm. The corresponding maximal displacement of the stress recovery zone and the low stress zone was 5.81 mm and 1.83 mm, respectively. The residual void of the compacted rock and coal fragments made from similar material was further compressed. The storage capacity nonlinearly decreased from 0.2409 m^3 to 0.2397 m^3. Ultimately, the storage coefficient of the coal mine underground reservoir was found to be 0.266.

(3) A four-dimensional spatial-temporal evolution law of storage coefficient in the coal mine underground reservoir (under joint interaction of water-rock and stress) was revealed. In space, the storage coefficient increased with height along the vertical direction of the coal mine underground reservoir, while it decreased with the distance from the boundary of the dam body in the horizontal direction. In time, the storage coefficient dynamically decreased with time.

Acknowledgements

This work was supported by the Youth Science Fund Program of National Natural Science Foundation of China (Grant No. 51704139), Open-end Research Fund of State Key Laboratory Coal Resources and Safe Mining (Grant No. SKLCRSM18KF011), and Open Fund of State Key Laboratory of Water Resource Protection and Utilization in Coal Mining (Grant No. SHJT-17-42.7).

References

Gu D.Z., Zhang Y., Cao Z.G., 2016. *Technical of water resource protection and utilization by coal mining in China.* Coal Science and Technology **44** (1), 1-7.

Fan L.M., Ma X.D., Ji R.J., 2015. *Progress in engineering practice of water-preserved coal mining in western eco-environment frangible area*. Journal of China Coal Society **40** (8), 1711-1717.

Luo L.P., 2010. *Research on the form mechanism of goaf water and its waterproof coal pillar dimension problem in coal mine*. China University of Mining and Technology-Beijing.

Gu D.Z., 2015. *Theory framework and technological system of coal mine underground reservoir*. Journal of China Coal Society **40** (2), 239-246.

Gao T.Y., 2015. *Numerical Simulation and optimal schedule of Daliuta-Mining-Area distributed underground reservoir*. Tsinghua University.

Peng X.N., Wu C.G., 1994. *Discussion on water storage rate of goaf in mine.* Coal science and technology **22** (9), 53-55.

Ballukraya P.N., Sharma K.K., 1991. Storage *coefficient measurement based on recovery data*. Ground Water, **29** (4), 495-498.

Sahni B.M., Harbhajan S.S., 1979. *Storage coefficients from ground-water maps.* Journal of the Irrigation and Drainage Division **105** (2), 205-212.

Arlai P., Lukjan A., Koch M., 2012. *3D groundwater model to estimate the dynamic groundwater storage in Viang Papao aquifers system*. Procedia Engineering **32**, 1221-1227.

Ordóñez A., Andrés C., Álvarez R., 2016. *Forecasting of Hydrographs to Simulate Long Term*

Recharge From Rivers in Numerical Models of Mining Reservoirs;Application to A Coal Mine in NW Spain [J]. River Research and Applications **32** (4), 552-560.

Oda M., Takemura T., Aoki T., 2002. *Damage growth and permeability change in triaxial compression tests of Inada granite.* Mech Mater **34** (6), 313-331.

Noiriel C., Renard F., Doan M-L., Gratier J-P., 2010. *Intense fracturing and fracture sealing induced by mineral growth in porous rocks.* Chem Geol **269** (3), 197-209.

Watanabe N., Ishibashi T., Ohsaki Y., Tsuchiya Y., Tamagawa T., Hirano N., Okabe H., Tsuchiya N., 2011. *X-ray CT based numerical analysis of fracture flow for core samples under various confining pressures*. Eng Geol **123** (4), 338-346.

Huang Q.X., Zhang W.Z., Hou Z.C., 2010. *Study of simulation materials of aquifuge for solid-liquid coupling.* Chinese Journal of Rock Mechanics and Engineering **29** (Suppl. 1), 2813-2818.

Wang K., Li S.C., Zhang Q.S., Zhang X., Li L.P., Zhang Q.Q., Liu C., 2016. *Development and application of new similar materials of surrounding rock for a fluid-solid coupling model test*. Rock and Soil Mechanics **37** (9), 2521-2533.

Fan G.W, Zhang S.Z, Zhang D.S, Chen M.W., 2016. *Development and application of a solid-liquid coupling physical experiment system for modeling mining-induced overburden movement*. Journal of Mining & Safety Engineering, **33** (5), 898-903.

Lian H.Q, Xia X.X, Ran W., Zhao Q.F., 2015. *Experimental research on water-resistance property of new-style fluid-solid coupling material for analogue simulation*. Coal Mining Technology **20** (1), 12-16.

Campoli A.A, Barton T.M, Van Dyke F.C., 1993. *Gob and gate road reaction to longwall mining in bump-prone strata* [M].US Department of the Interior, Bureau of Mines.

Wilson A.H., 1983. *The stability of underground workings in the soft rocks of the coal measures* [J]. International Journal of Mining Engineering **1** (2), 91-187.

King H.J., Whittaker B.N., 1970. *A review of current knowledge on roadway behavior, especially the problems on which further information is required* [C]. Proceedings of the Symposium on Strata Control in Roadway. London: IME 1971, 73-90.

Yavuz H (2004) *An estimation method for cover pressure re-establishment distance and pressure distribution in the goaf of longwall coal mines* [J]. International Journal of Rock Mechanics and Mining Sciences **41** (2):193-205.

Wang Z.Y., ,Liu H.Q., 1993. *Consistency between stress in goaf area, movement law of overlying strata and stress effect of roof and floor rock*. Coal Mining Technology (1), 38-44.

Liang B., Wang BF., Jiang LG., Li G., Li CY., 2016. *Broken expand properties of caving rock in shallow buried goaf.* Journal of China University of Mining & Technology **45** (3), 475-482.

Wang W.X., Wang S.W., Liu H.N., Jiang T., Ren M., 2017. *The space and time characteristics of the cover stress re-establishment of the fractured rock mass in the goaf after coal mining*. Journal of Mining & Safety Engineering **34** (1),127-133.

Palchik V., 2015. *Bulking factors and extents of caved zones in weathered overburden of shallow abandoned underground workings*. International Journal of Rock Mechanics and Mining Sciences **79**, 227-240.

Groccia C., Cai M., Punkkinen A., 2016. *Quantifying rock mass bulking at a deep underground nickel mine*. International Journal of Rock Mechanics and Mining Sciences **81**,1-11.